International Forum on Aeroelasticity and Structural Dynamics
IFASD 2024
17-21 June 2024, The Hague, The Netherlands

THE EFFECT OF AERODYNAMIC INTERACTIONS ON AEROELASTIC STABILITY IN WING-PROPELLER SYSTEMS

Nils Böhnisch[1], Carsten Braun[1], Vincenzo Muscarello[2], Pier Marzocca[2]

[1]FH Aachen University of Applied Sciences
Hohenstaufenallee 6, 52146 Aachen, Germany
boehnisch@fh-aachen.de
c.braun@fh-aachen.de

[2]Royal Melbourne Institute of Technology
124 La Trobe St, Melbourne VIC 3000, Australia
vincenzo. muscarello@rmit.edu.au
pier.marzocca@rmit.edu.au

Keywords: Wing-Propeller Model, Flutter, Aerodynamic Interaction

Abstract: This paper presents initial findings from aeroelastic studies conducted on a wing-propeller model, aimed at evaluating the impact of aerodynamic interactions on wing flutter mechanisms and overall aeroelastic performance. Utilizing a frequency domain method, the flutter onset within a specified flight speed range is assessed. Mid-fidelity tools with a time domain approach are then used to account for the complex aerodynamic interaction between the propeller and the wing. Specifically, open-source software DUST and MBDyn are leveraged for this purpose. This investigation covers both windmilling and thrusting conditions of the wing-propeller model. During the trim process, adjustments to the collective pitch of the blades are made to ensure consistency across operational points. Time histories are then analyzed to pinpoint flutter onset, and corresponding frequencies and damping ratios are meticulously identified. The results reveal a marginal destabilizing effect of aerodynamic interaction on flutter speed, approximately 5%. Notably, the thrusting condition demonstrates a greater destabilizing influence compared to windmilling. These comprehensive findings enhance the understanding of the aerodynamic behavior of such systems and offer valuable insights for early design predictions and the development of streamlined models for future endeavors.

1 INTRODUCTION

The integration of electric propulsion in aircraft design, made possible by electrification, has provided numerous advantages. Next-generation aircraft configurations can benefit from electric propulsion in terms of aerodynamic efficiency and simplicity [1, 2], leading to the development of distributed electric propulsion systems (DEPs), where the propulsion can be placed at various locations. The relatively light weight of electric propulsion allows for propellers to be distributed along the wingspan, taking advantage of their high efficiency at low speeds [3]. However, these mass-optimized structures are inherently flexible. Combined with the presence of rotating propellers, the dynamic behavior becomes a critical factor, particularly for aeroelastic aspects. In the context of DEP configuration, the main aeroelastic phenomena are wing flutter and propeller whirl flutter. While wing flutter is a well-examined phenomenon, whirl flutter is receiving renewed attention due to novel configurations. The foundational focus and development of suitable estimation procedures emerged in the 1960s [4, 5]. A straightforward structural

model by Reed and Bland was developed during this period, and the associated aerodynamics were described analytically [4]. This work laid the groundwork for whirl flutter theory.
The evaluation of aeroelasticity in next-generation aircraft designs poses a critical challenge for engineers. To address this challenge, a thorough understanding of the aeroelastic behavior of such configurations is essential, followed by the development of reliable aeroelastic prediction methods. Gaining a detailed understanding of the aeroelastic behavior needs examining the complex interactions between the wings and propellers, taking into account factors like propeller mounting stiffness, wing dynamics, propeller performance, and aerodynamic interactions. It is therefore not surprising that extensive research has been conducted recently on aeroelastic instabilities concerning wing flutter and propeller whirl flutter. An enhanced method for unsteady propeller aerodynamics used for whirl flutter was presented in [6] and compared to low- and mid-fidelity methods in [7]. The stabilizing effect of the propeller aerodynamic torque on whirl flutter was investigated in [8].
For coupled wing-propeller models, structural interactions between the wing and propeller were studied using assumed mode shapes in [9] and recently investigated by the authors [10, 11]. The influence of gyroscopic effects of rotating masses was highlighted in [12, 13]. In terms of aerodynamic interaction, it is known that aircraft designs with a DEP have a positive influence on the lift-drag ratio and overall performance [1, 2]. However, several questions remain unanswered. For instance, the effect of aerodynamic interaction between propellers and the wing on aeroelastic behavior requires investigation. Preliminary studies have indicated that both the thrust generated by propellers [14, 15] and the aerodynamic effects of propellers on the flow around the wing [16] influence the aeroelastic stability. Further, the aerodynamic interaction was discovered to be slightly destabilizing for whirl flutter cases [17]. This study aims to enhance the understanding of the flutter mechanism in wing-propeller models, with a specific focus on investigating the influence of aerodynamic interference between the propeller and the wing on wing flutter. To achieve this, a wing-propeller model will be utilized, and the mounting stiffness will be modified to induce wing flutter[11]. The paper is structured as follows: The first section outlines the methodology and the analytical tool used for analyzing the aeroelastic model. In the subsequent section, the wing and propeller models are presented, along with the initial validation of the chosen approach. This is followed by the presentation and discussion of the results. Finally, conclusions are drawn.

2 TOOLS AND MODELING APPROACHES

The coupled wing-propeller model can be investigated through different methods. In the present work, two primary approaches are used: frequency domain and coupled multibody - mid fidelity aerodynamic simulations. For the coupled analysis, a time-marching procedure is employed to perform simulations at different freestream velocities and to identify the critical aeroelastic speed. This approach offers high accuracy and flexibility, particularly when a workflow for fluid-structure interaction analysis is established. However, it requires more computational power and time due to the complexity of the calculations. On the other hand, frequency-domain simulations provide faster results by solving an eigenvalue problem at distinct freestream velocities to determine mode shapes, frequencies, and damping ratios. However, it requires prior knowledge of unsteady aerodynamics for harmonic motion. As a consequence the results are only physically correct at the flutter point.
To overcome some of the limitations, this paper employs both approaches. For the frequency-domain simulations, an in-house toolbox (SDBox) is used. This toolbox provides the necessary capabilities for efficient analysis and delivers initial results on flutter points, natural frequencies, damping ratios and mode shapes.

SDBox was developed in MATLAB. It was designed for predicting flutter speeds of propellers, wings, and wings coupled with multiple propellers and was presented by the authors in [10, 18]. The flexibility of the wing is modeled using beam elements based on a Timoshenko description. The propellers are attached to the wing's elastic axis via rotational springs that represent a simplified flexible pylon system allowing rotations in pitch and yaw. Wing aerodynamics are modeled using the Doublet Lattice Method (DLM). Propeller aerodynamics are modeled by the inclusion of propeller stability derivatives as described in [5, 19]. However, instead of using an analytical description of the derivatives, an enhanced, full unsteady approach is applied to identify the propeller aerodynamic derivatives as described in [6, 7]. The coupled system is described by the classical flutter equations and finally solved with the p-k method. Aerodynamic interaction is neglected in this framework. SDBox has proven powerful and efficient in the fast prediction of flutter speeds and has been successfully validated in [20].
For the time-domain simulations, a coupled toolchain consisting of MBDyn [21] and DUST [22] is employed. MBDyn is a multibody dynamics tool that offers the capability to model complex mechanical systems. Nonlinear dynamics of rigid and flexible bodies can be simulated, connected by kinematic constraints. The equations of motion are formulated in differential algebraic form, which are solved numerically. MBDyn also features an aerodynamic module that incorporates strip theory in conjunction with a dynamic inflow model with three inflow states [23, 24]. DUST, on the other hand, is an aerodynamic tool that relies on potential flow theory. It employs a free wake description with vortex particles. This approach allows for more accurate modeling of complex geometries by offering multiple elements, such as lifting lines for slender lift-generating surfaces, vortex lattice elements, and surface panels. To facilitate the coupling of MBDyn and DUST for aeroelastic simulations the open-source tool PreCice [25] is utilized [26]. PreCice provides a tight coupling scheme, enabling the exchange of information between the two solvers in real time. This coupling framework enhances the accuracy and efficiency of the simulations by enabling the seamless interaction between the multibody and the aerodynamic solvers.
The primary focus of this paper is to investigate the influence of aerodynamic interference between the propeller and the wing on flutter. To achieve this target, various analysis approaches are used. An overview is given in Table 1. The analysis is driven by SDBox, to establish an

Table 1: Overview fo analysis approaches.

Name	**Structure**	**Aerodynamic**			**Domain**
		Propeller	**Wing**	**Interaction**	
SDBox	Beam	Derivatives	DLM	NO	Frequency
Hybrid	MBDyn: Beam	MBDyn: Strip Theory + Inflow Model	DUST: Surface Panels	NO	Time
Fully Coupled	MBDyn: Beam	DUST: Lifting Line	DUST: Surface Panels	YES via particles	Time

initial flutter prediction. Starting from these results, the velocity range of interest is used for the time-marching simulations. Subsequently, two distinct time-domain approaches are conducted. The first, named "Hybrid", neglects the wing-propeller aerodynamic interference, while the second approach, referred to as "Fully Coupled" does. The comparison of the respective flutter analysis results provides a statement about the influence of the aerodynamic interaction on aeroelastic stability. A detailed description of the modeling is presented in the next section.

3 MODELS AND VALIDATION

3.1 Wing and Propeller Model

The wing model used in this study corresponds to the one previously described in [18]. It comprises a rectangular wing with a total aspect ratio of 9.12. The structural mass of the wing is approximately 102 kg. In the absence of the attached propeller, the wing's eigenfrequencies and damping ratios in the wind-off condition have been calculated and can be found in Table 2. An aeroelastic investigation was conducted for the standalone wing using SDBox and DUST

Table 2: Eigenfrequencies and damping ratios for standalone wing.

Mode	Description	Frequency, Hz	Damping Ratio, -
1	First bending	6.75	0.02
2	First torsion	10.96	0.03
3	Second torsion	13.79	0.04
4	Second bending	30.33	0.10

coupled with MBDyn. The comparison of the flutter point in terms of velocity and frequency showed excellent agreement, as reported in [18] and summarized in Table 3.

Table 3: Flutter speed and frequency for standalone wing.

	SDBox	DUST + MBDyn
Flutter Speed, $\mathrm{m\,s^{-1}}$	93	95
Flutter Frequency, Hz	9.07	8.93

The propeller employed throughout the proposed study is a four-bladed propeller with a diameter of 1.8m. The blade geometrical parameter are presented in Fig. 1 showing a linear twist and a constant chord distribution. Inertia properties are attributed to all the propeller blades

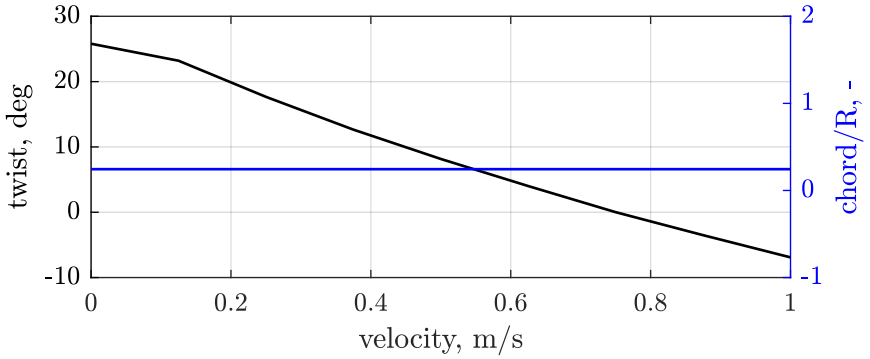

Figure 1: Twist and chord distribution of propeller blade.

(total 8.8 kg) and an electric motor (25 kg) situated slightly ahead of the propeller hub. The pylon support and propeller blades are assumed to be rigid, while the mounting stiffness at the propeller's pivoting point allows for pitch and yaw rotation modeling a flexible pylon system [8]. Consequently, a typical 2-degrees-of-freedom model for propeller whirl flutter, consistent with state-of-the-art practices, has been established. For simplicity, the propeller blades are assumed to have a symmetrical NACA0012 airfoil. To facilitate the analysis in SDBox, unsteady propeller aerodynamics were precalculated by employing lifting line theory and wake particles in DUST. Determination of the unsteady propeller derivatives for various harmonic excitation frequencies was achieved using transfer functions with the methods explained in [6, 7].

3.2 Coupled Multibody - Mid Fidelity Aerodynamic Wing-Propeller Model

This section describes the modeling for the wing-propeller system. The model used for SDBox is the same as presented in [11] and the model used for the Hybrid and Fully Coupled approach in MBDyn and DUST is described below. As given in table 1, the structural components of the system are modeled in MBDyn. This includes the wing and the propeller. An overview of the model set up is given in Fig. 2. The wing elastic properties are modeled using three-node beam

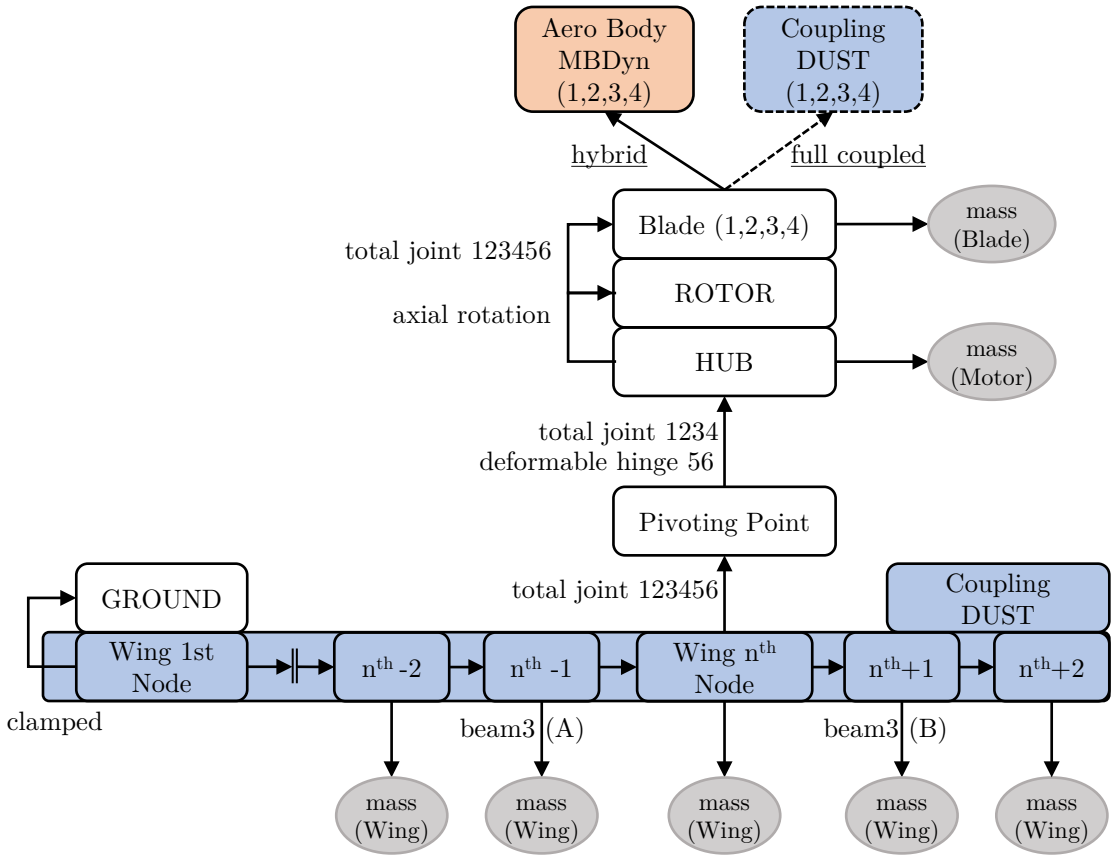

Figure 2: Chart of coupled propeller-wing model in MBDyn.

elements. Structural damping for the wing is modeled with a proportional stiffness factor of 1%. The root of the wing is clamped. Inertia properties of the wing are modeled using lumped masses at each node, accounting for the offset between the elastic axis and the center of gravity axis. In total 41 nodes and 20 beam elements are used. The propeller is attached at 50% semi-span. The pivoting point of the propeller is rigidly connected to the n-th node at a distance l in front of the elastic axis (i.e.: towards the leading edge). The propeller hub is connected to the pivoting point through two joints: a total joint and a deformable hinge. The deformable hinge represents the rotational stiffnesses in yaw and pitch. Damping effects are neglected in this joint. The rotor node is located at the same position as the hub nodes. They are both are connected via an axial rotation constraint, which enforces the rotation of the propeller. Additionally, four nodes are rigidly attached to the rotor node, representing the blades. The mass of the motor is connected to the hub node (non-rotating mass). Propeller blades are assumed to be rigid. The corresponding mass/inertia is lumped at the blade center of mass. For the hybrid approach, each blade is also connected to an aerodynamic body, which represents the aerodynamic model in MBDyn. As previously mentioned , this model incorporates a propeller dynamic inflow and correction factors such as tip loss correction. The chord and twist distributions are specified as

input parameters. For the Fully Coupled approach, the nodes of the propeller are selected for coupling with DUST.
Propeller aerodynamics in DUST are modeled using lifting line elements (see Fig. 3). The aero-

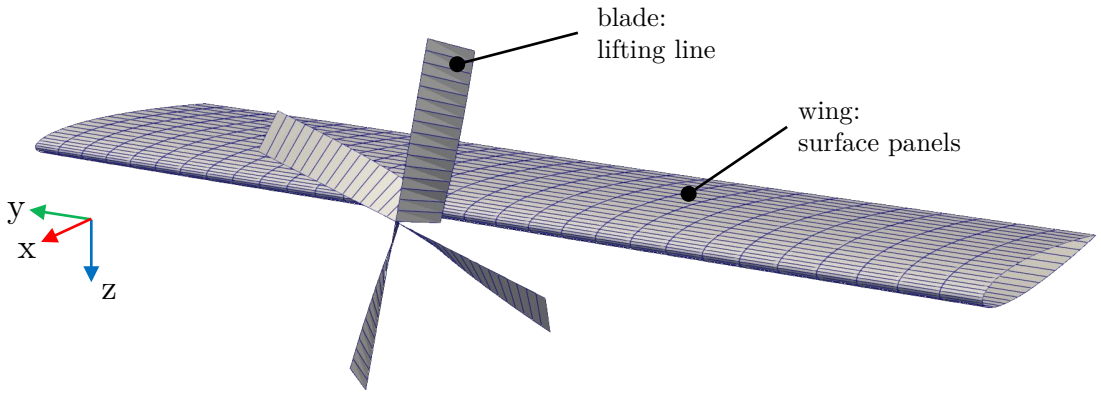

Figure 3: DUST aerodynamic model for wing and propeller.

dynamics of the wing are modeled in DUST for both approaches. For each coupling node, displacements, velocities, and accelerations are exchanged using the PreCice coupling framework [25]. Surface panels are employed to represent the wing's geometry. The wing is discretized with 30 panels in the span direction and 20 panels in the chord direction. To accurately capture the curvature of the leading edge, the chord distribution is discretized using a half-cosine function.

3.3 Operational Conditions and Trim Process

Before running the flutter analysis, a trim condition needs to be defined. The trim condition is primarily defined by the propeller operational point, while the wing angle of attack and the lift generated are not considered as trim parameters. This decision is based on the use of a symmetrical airfoil with zero angle of attack, and the assumption that the additional lift from the propeller wake is expected to be small. Further, the wing airfoil choice does only minor affect the aeroelastic behavior of a wing. Therefore, only the propeller trim is considered in this work. This paper focuses on two distinct conditions. The windmilling condition is chosen

Table 4: Operational condition under investigation.

Name	Requirement	Rot. Speed, rpm
Windmilling	$Q = 0$ N m	2500
Thrusting	$T = 750$ N	2500

because it represents the most critical condition with respect to propeller whirl flutter [27]. Since the influence of the aerodynamic interaction of the propeller and wing on flutter is still an object of study, a thrusting condition is also considered. In this case, the thrust required by the aircraft is chosen as the trim point condition. Generally, the propeller's operational point is a function of the freestream velocity, rotational speed (i.e., the propeller advance ratio), and the collective pitch angle of the blades. A constant rotational speed of the propeller is selected to maintain a constant angular momentum, while the freestream velocity is given by the time marching approach. Consequently, the only parameter left to achieve a trim condition is the collective pitch of the blades, which will be used within this study.

3.4 Tuning and Validation of the Standalone Propeller Model

In order to ensure consistency in the aerodynamic modeling of the propeller, a comparison was conducted based on the two different time-domain analysis approaches. This was achieved by examining the performance curves for the standalone propeller without the presence of the wing. The thrust and torque with reference to the advance ratio for the simulations conducted using DUST and MBDyn are presented in Fig. 4, respectively. The MBDyn model was tuned to align with the results obtained from DUST, as it is the higher order method. As observed, the curves exhibit a very good match, indicating a consistent aerodynamic modeling approach. Additionally, the classical stability map for the standalone propeller was created using the SD-

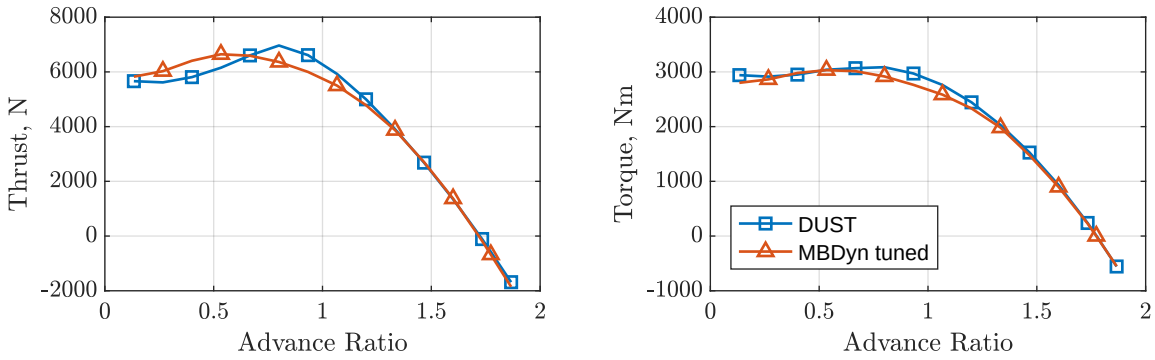

Figure 4: Thrust (left) and torque (right) vs. advance ratio (J) for a collective pitch of 38.2 deg.

Box for a freestream velocity of 133 $\mathrm{m\,s^{-1}}$ and windmilling condition (see Fig. 5). As seen, the largest required stiffness is found to be 188,000 $\mathrm{N\,m\,rad^{-1}}$ at isotropic stiffness conditions. The same conditions were analyzed using both time-domain approaches, i.e. Hybrid and Fully

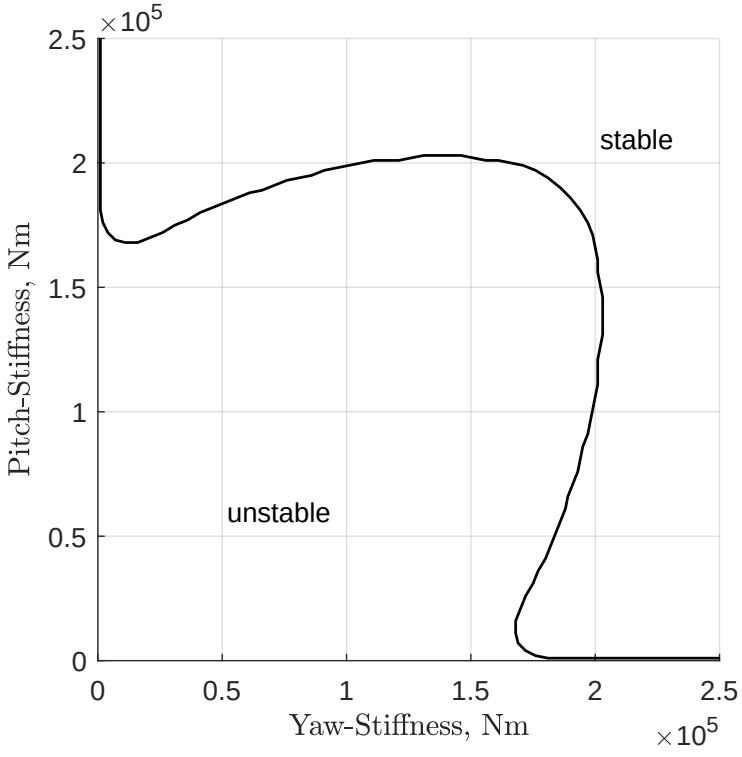

Figure 5: Stability map for standalone propeller ($V = 133\ \mathrm{m\,s^{-1}}$, $rpm = 2500$, and collective pitch $\beta = 38.2\ ^\circ$).

Coupled. The time histories were post-processed using the Matrix Pencile Estimation (MPE) to extract eigenfrequencies and damping ratios. The results are summarized in Table 5, further supporting the aerodynamic consistency between the two different analysis approaches.

Table 5: Comparison of eigenfrequencies and damping ratios for standalone propeller time simulations. Freestream velocity of 133 $\mathrm{m\,s^{-1}}$ and isotropic stiffness of 188,000 $\mathrm{N\,m\,rad^{-1}}$.

	Hybrid		Fully Coupled	
Mode	freq. , Hz	damp., %	freq. , Hz	damp., %
Backward Whirl	22.62	0.02	22.20	0.03
Forward Whirl	42.22	3.00	42.09	2.86

3.5 Steady Aerodynamic Interaction

Since the aerodynamic interaction effect is of particular focus in this study, a Fully Coupled time-domain simulation for a wing-propeller system at zero angle of attack with rigid structure is performed. The propeller operates in thrusting case. The pressure distribution of this simulation is depicted in Fig. 6 for an ISO-view (a) and a top-view (b). In the former, the wake

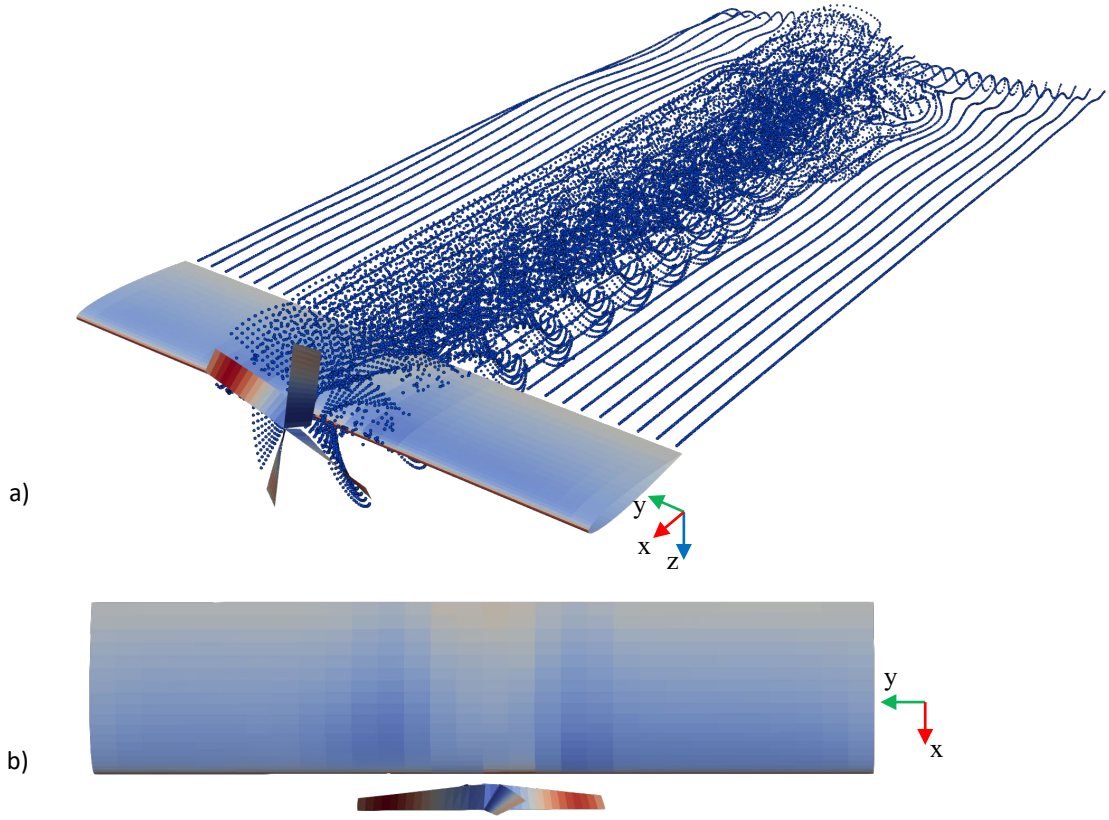

Figure 6: Pressure distribution and particles of Fully Coupled simulation. a: ISO-View, b:top-view.

particles are displayed and the propeller helix and the wing wake particles are visible. Note that no tip vortexes are present due to the symmetrical airfoil at zero angle of attack. According to literature [28, 29], the aerodynamic interaction leads to pressure zones on the wing due to the helix wake. These zones leads to a slightly increase or decrease in local pressure based on the rotational direction of the propeller. The c_L distribution of the wing along the dimensionless semispan is presented in Fig. 7. The behavior is similar to those found in the literature [28, 29] with the low c_L values for the down-moving half (left side) of the propeller disk and a positive

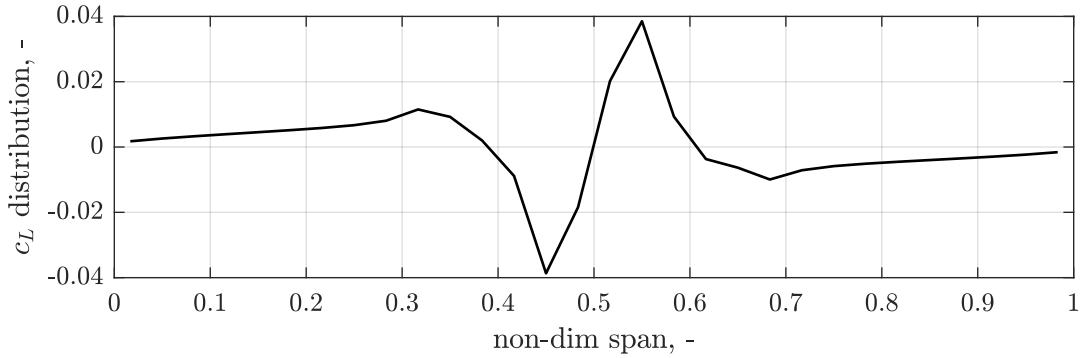

Figure 7: c_l distribution of wing due to propeller in thrusting condition.

c_L on the up-moving half (right side) of the propeller disk. At root and tip, the c_L reduced to zero as expected.

4 RESULTS

In this section, the aeroelastic stability analysis results obtained with the Hybrid and the Fully Coupled approach are discussed and compared. In the following, the free stream velocity is varied, and the wing-propeller response simulated. Frequencies and damping ratios are extracted using the MPE method. First the flutter prediction with SDBox is presented followed by the trim results. Finally, stability analysis results are shown and discussed for both operational conditions.

4.1 Preliminary Flutter Prediction and Trim Results

To establish an initial velocity range for flutter analysis, SDBox was employed to predict critical speeds for the wing-propeller system, with the propeller positioned at 50% of the semispan. The mounting stiffness of the propeller is set to 40,000 $\mathrm{N\,m\,rad^{-1}}$. The relatively low mounting stiffness is intentionally chosen to induce flutter within a realistic velocity range. In general, such low stiffness values can be considered a failure case of the pylon, where structural integrity is reduced. The propeller aerodynamics are modeled with precalculated unsteady propeller derivatives in windmilling condition [11]. The resulting flutter curves are depicted in Fig. 8. As illustrated by the red marker, flutter occurs at approximately 133 $\mathrm{m\,s^{-1}}$ triggered by mode 3. The corresponding flutter mode shape is presented in Fig. 9 showing a strong coupling between the out-of-plane bending and the torsional motion of the wing. The propeller exhibits an elliptical backward whirl motion due to precession. This flutter mechanisms is refereed to wing-dominant flutter [11]. It should be highlighted that whirl flutter is not present here, even though the mounting stiffness is smaller than the identified required stiffness for the standalone propeller (see Fig. 5). This behavior can be attributed to the stabilizing influence of the elastic wing on whirl flutter [11]. In the case of a rigid wing, whirl flutter would indeed occur.
The predicted flutter speed was used to define the velocity range of interest for the time-marching analyses and for the trimming process. The required collective pitch angle for the propeller blades as a function of the freestream velocity was calculated based on precalculated performance curves of the standalone propeller (Hybrid approach) and the wing-propeller system (Fully Coupled approach). The trim results are shown in Fig. 10. The solid curves represents the windmilling condition, and the dashed curves represents the thrusting condition. As expected, with increasing free stream velocity, the pitch angle increases as well. The collective pitch angles for the thrusting case are higher compared to the windmilling condition. It is interesting to note, that the trim angles for the Fully Coupled simulation (blue lines) are

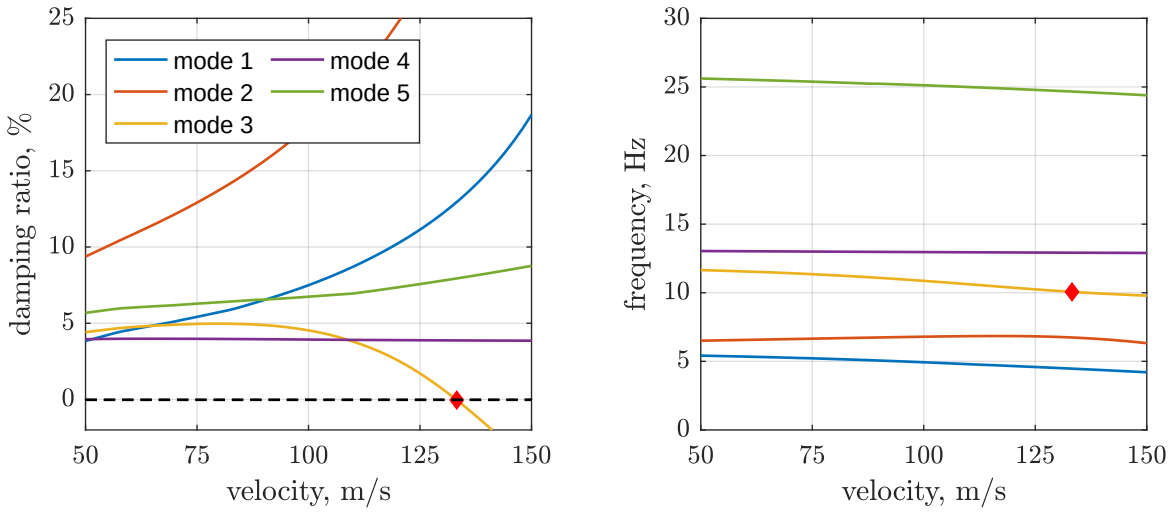

Figure 8: Flutter curves (v-g: left & v-f: right) for propeller at 50% span with 40,000 $\mathrm{N\,m\,rad^{-1}}$ mounting stiffness.

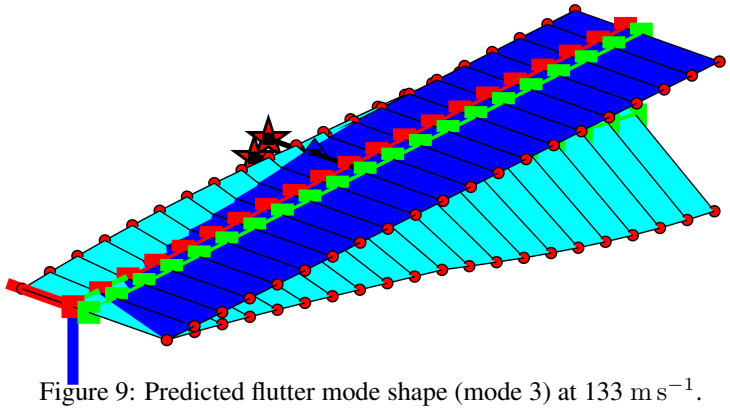

Figure 9: Predicted flutter mode shape (mode 3) at 133 $\mathrm{m\,s^{-1}}$.

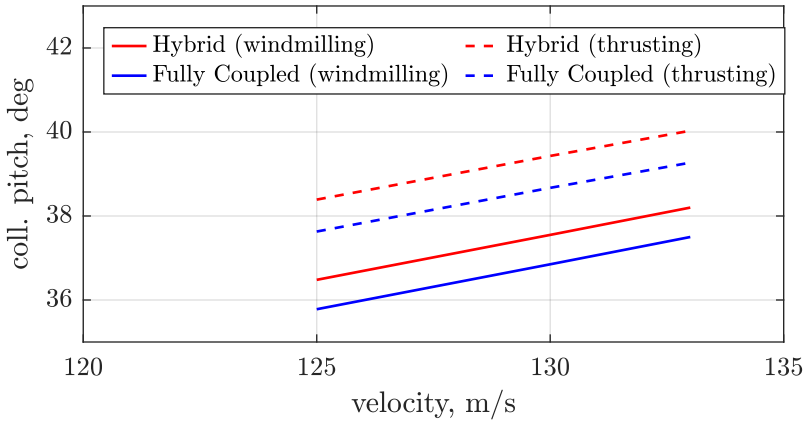

Figure 10: Trim results to obtain desired operational condition for Hybrid and Fully Coupled approach.

constantly smaller compared to the Hybrid approach (red lines). This effect is attributed to the aerodynamic interaction between the propeller and wing.

4.2 Stability Results

The stability results are presented in this section. The system is initially excited by a blended impulse force at the wing tip located before the elastic axis. With that, out-of-plane bending and

torsional modes are excited. The blended impulse is applied within 2 ms and with an amplitude of 12 kN to ensure an excitation up to 30 Hz. The free response of the system, encompassing both aerodynamics and structural dynamics, was subsequently tracked. Three distinctive free stream velocities were simulated for both the Hybrid and the Fully Coupled approaches. The results for the windmilling condition are depicted in Fig. 11. Each plot represents the dynamic

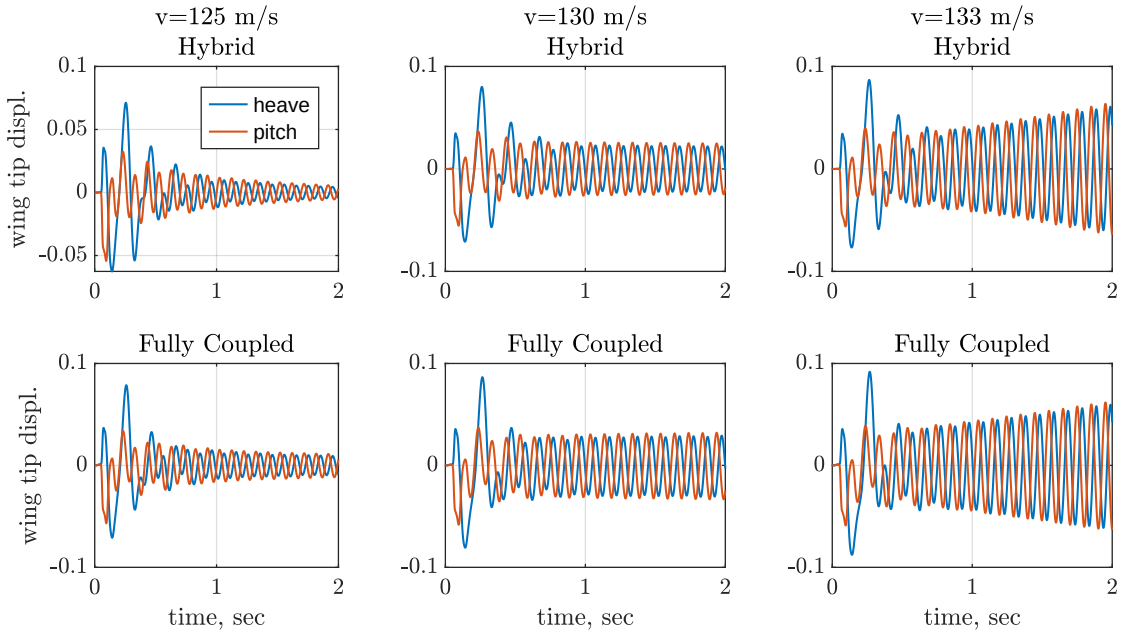

Figure 11: Time histories of wing tip node for Hybrid and Fully Coupled approach in windmilling condition.

response of the wing's tip node in pitch and heave. The figures on the top illustrate the response of the Hybrid approach, while the figures on the bottom display the response of the Fully Coupled approach. At the beginning of all simulations, the transient behavior due to the blended impulse is observable. After a few milliseconds, most of the excited modes are damped due to aerodynamic effects. Subsequently, the poorly damped dynamic survives, and is used to identify the dynamic response. A preliminary stability assessment can be performed by visual inspection of the time histories. For both simulation approaches, a clearly unstable behavior is observed at a free stream velocity of 133 $\mathrm{m\,s^{-1}}$. At 125 $\mathrm{m\,s^{-1}}$ and 130 $\mathrm{m\,s^{-1}}$ the measured responses exhibit stable and indifferent behavior, respectively. The results of the MPE in form of eigenfrequencies and damping ratios are summarized in Table 6. It should be noted that the MPE

Table 6: Frequencies and damping ratio's of the critical mode for simulations in windmilling condition.

	SDBox		Hybrid		Fully Coupled	
velocity, $\mathrm{m\,s^{-1}}$	freq. , Hz	damp., %	freq. , Hz	damp., %	freq. , Hz	damp, %
125	10.25	1.70	10.10	1.30	10.11	0.57
130	10.13	0.69	9.98	0.07	9.98	-0.09
133	10.07	0.02	9.92	-0.71	9.91	-0.55

method often fails to accurately predict eigenfrequencies and damping ratios for highly damped modes and thus only the poorly damped modes after the transient phase are identified. The comparison between the simulation approaches revealed no significant differences, however, the Fully Coupled simulations returns a slightly smaller flutter speed compared to the Hybrid approach and SDBox. No large differences between the analysis approaches can be observed, leading to the conclusion that the aerodynamic interaction effects in windmilling condition are

only minor in terms of stability. The time histories for the same freestream velocities, but for the thrusting propeller are presented in Fig. 12. Again, stable and unstable behaviors are clearly visible at 125 $\mathrm{m\,s^{-1}}$ and 133 $\mathrm{m\,s^{-1}}$ for both simulation approaches, respectively. Consequently, flutter is again covered within the velocity range considered. In contrast to the windmilling

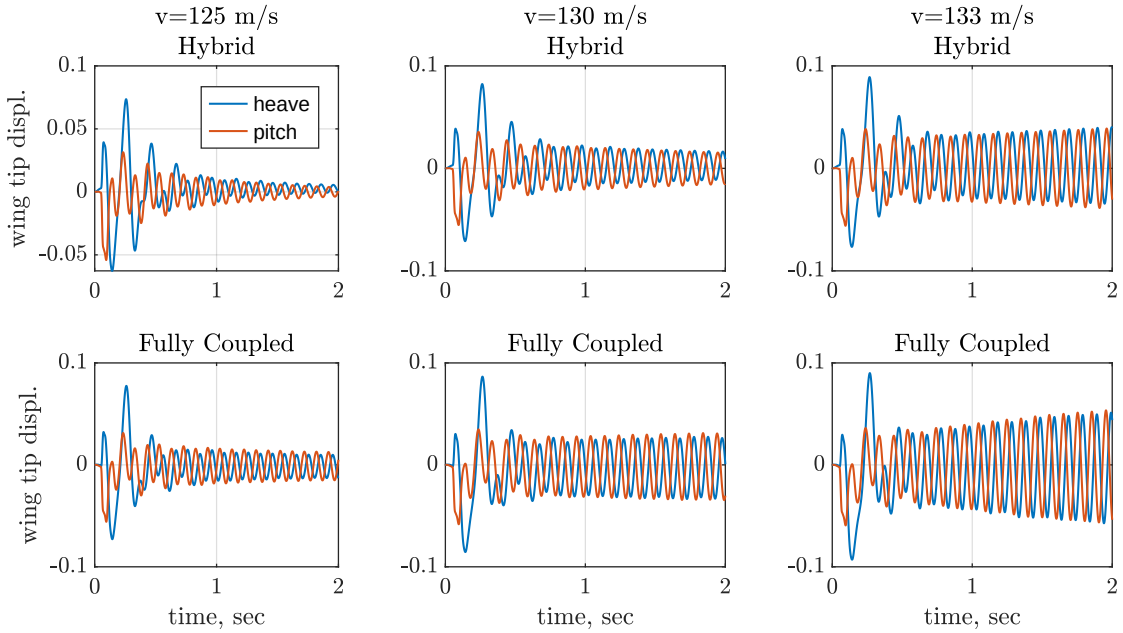

Figure 12: Time histories of wing tip node for Hybrid and Fully Coupled approach in thrusting condition.

condition, the comparison between the Hybrid and Fully Coupled approaches reveals more pronounced differences in the response. Indeed, the Fully Coupled approach appears to be less stable across all velocities compared to the Hybrid approach. These results are confirmed by the MPE method (see table 7). The Fully Coupled approach returns an unstable condition at

Table 7: Frequencies and damping ratio's of the critical mode for simulations in thrusting condition.

	SDBox		Hybrid		Fully Coupled	
velocity, $\mathrm{m\,s^{-1}}$	freq. , Hz	damp., %	freq. , Hz	damp., %	freq. , Hz	damp, %
125	10.12	2.06	10.07	1.61	10.10	0.35
130	10.00	1.01	9.94	0.48	9.95	-0.19
133	9.93	0.31	9.87	-0.29	9.89	-0.44

130 $\mathrm{m\,s^{-1}}$. Consequently, the influence of the aerodynamic interaction on flutter is stronger in case of a thrusting operational condition. It is believed that this effect can be attributed to the induced velocities of the propeller since it is higher in thrusting case compared to windmilling. This leads to higher local dynamic pressures and in turn to higher aerodynamic loads.
In summary, one can discern trends in damping and frequencies across the four combinations of time-domain approaches and trim conditions depicted in classical flutter curves. These trends are illustrated in Fig. 13. The predicted flutter mode 3 by the frequency method (SDBox) is also included for both trim condition, while in case of the thrusting propeller, the corresponding propeller derivatives has been used. Yellow, red-crossed, and blue-circled lines represents the SDBox, Hybrid, and Fully Coupled approach respectively. Solid lines were obtained for the windmilling condition and dashed lines for the thrusting condition. The frequency of the critical mode aligns well with the prediction made by SDBox for mode 3, regardless the trim condition. Additionally, the occurrence of flutter within the considered velocity range is ac-

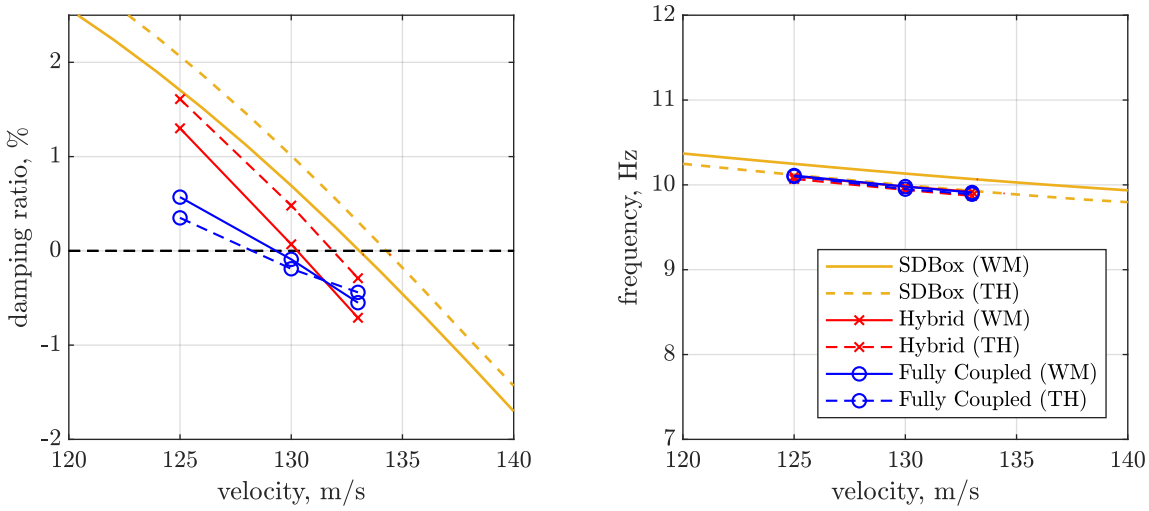

Figure 13: Damping and frequency trend for unstable mode for all three simulation approaches.

curately captured. Across all time domain approaches, it is observed that the flutter speed is slightly overpredicted by SDBox. In contrast, the Fully Coupled approach (blue lines) always predicts the lowest flutter speed, irrespective of the trim condition. The largest difference between SDBox and Fully Coupled approach in flutter speed for this particular model is 4.5% and 3.3% between Hybrid and Full-Coupled approach for the thrusting case. Again, this is believed due to the higher induced velocities. Interestingly, it is noted that in the case of the Hybrid and SDBox approach, the windmilling condition is predicted to be more critical than the thrusting condition. With the Fully Coupled approach, however, the situation is reversed. It is assumed that this can be assigned to the propeller torque which potentially stabilized the wing-propeller system since it is known to have a stabilizing contribution on whirl motion [8]. Following this, the aerodynamic interactions between wing and propeller seems to counteracting this, leading to a reduced flutter speed for a thrusting propeller (see Fully Coupled approach). In addition, the slope of the damping behavior of the critical mode is flatter for the Fully Coupled approach than for the Hybrid approach and SDBox.

5 CONCLUSIONS

This paper investigates the effects of aerodynamic interactions on aeroelastic stability within a wing-propeller system. The focus is primarily on a flutter mechanism originating from the wing. A baseline model was established featuring a flexible wing and a mid-semispan-mounted propeller with a flexible pylon and rigid blades. The stiffness properties of the pylon represent a failure case scenario. Flutter for this model was predicted using a frequency domain method neglecting the aerodynamic interaction at a speed of 133 $\mathrm{m\,s^{-1}}$. To assess the impact of aerodynamic interaction, coupled fluid structure time-domain simulation were performed. Structural modeling was conducted using a multi-body dynamics code (MBDyn). For the aerodynamic modeling, two different simulation approaches were defined. In the first approach (Hybrid), the propeller aerodynamics were modeled separately from the wing aerodynamics, neglecting interference. Specifically, propeller aerodynamics were modeled using an a blade element model together with a 3 states dynamic inflow model within MBDyn, while wing aerodynamics were modeled using a 3D panel method with a free wake particle description (DUST). In the second approach (Fully Coupled), both elements, propeller and wing, were aerodynamically modeled in DUST, with the propeller modeled using lifting line elements. The particle wake descrip-

tion in DUST allows to consider aerodynamic interactions between the propeller and the wing. In both simulation approaches, a time-marching scheme was applied to find the flutter point. Two trim points were selected: (1) windmilling and (2) thrusting case. The former is known to be most critical for whirl flutter, and the latter represents a typical trim condition in steady level flight. Trim conditions were ensured by varying the collective pitch of the propeller while holding the rotational speed constant at 2500 rpm. Time histories were extracted, and eigenfrequencies and damping ratios for the critical mode were extracted using the MPE method. The main findings of these studies revealed:

- The consideration of aerodynamic wing-propeller interaction effects in stability analysis leads to reduced flutter speeds for both windmilling and thrusting cases.
- Neglecting aerodynamic interference, the windmilling condition returns the smallest flutter boundaries. This behavior is also seen in the majority of the cases discussed in literature for the standalone propeller.
- Including aerodynamic interference, the thrusting condition returns the smallest stability boundaries which is assumed due to higher local dynamic pressures on the wing induced by the propeller.
- The difference in the flutter speed for the analyzed configuration is less than 5% between the frequency domain approach without aerodynamic interaction and the fully coupled approach. Therefore, the frequency domain approach is preferable for preliminary analyses. It is faster compared to time marching analyses and provides accurate results, although the results are not conservative in terms of flutter speed.

Further studies will overcome the limitations concerning lift generating wing (asymmetrical airfoil) and non-zero angle of attacks and will be extended to investigate the effect of aerodynamic interactions on whirl flutter mechanisms for wing-propeller systems. The effects of multiple propellers will also be investigated, as the approach presented in this study has proven to be suitable. This research aims to enhance the understanding of aeroelastic behavior and provide valuable insights for the structural design of multiple-propeller aircraft.

REFERENCES

[1] de Vries, R., and Vos, R., "Aerodynamic Performance Benefits of Over-the-Wing Distributed Propulsion for Hybrid-Electric Transport Aircraft," *AIAA SciTech 2022 Forum*, American Institute of Aeronautics and Astronautics, Reston, Virginia, 2022. doi: 10.2514/6.2022-0128.

[2] Stoll, A. M., Bevirt, J., Moore, M. D., Fredericks, W. J., and Borer, N. K., "Drag Reduction Through Distributed Electric Propulsion," *14th AIAA Aviation Technology, Integration, and Operations Conference*, American Institute of Aeronautics and Astronautics, Reston, Virginia, 2014. doi:10.2514/6.2014-2851.

[3] Heeg, J., Standford, B. K., Kreshock, A., Shen, J., Hoover, C. B., and Truax, R., "Whirl Flutter and the Development of the NASA X-57 MAXWELL," *International Forum on Aeroelasticity and Structural Dynamics*, 2019.

[4] Reed, W. H., and Bland, S. R., "An Analytical Treatment of Aircraft Propeller Precession Instability," Tech. Rep. Technical Note D-659, Langley Reserach Center, Washington, USA, 1961.

[5] Houbolt, J. C., and Reed, W. H., "Propeller-Nacelle Whirl Flutter," *Journal of the Aerospace Sciences*, Vol. 29, No. 3, 1962, pp. 333–346. doi:10.2514/8.9417.

[6] Koch, C., "Whirl Flutter Stability Assessment Using Rotor Transfer Matrices," *International Forum on Aeroelasticity and Structural Dynamics 2022*, 2022.

[7] Koch, C., Böhnisch, N., Verdonck, H., Hach, O., and Braun, C., "Comparison of Unsteady Low- and Mid-Fidelity Propeller Aerodynamic Methods for Whirl Flutter Applications," *Applied Sciences*, Vol. 14, No. 2, 2024, p. 850. doi:10.3390/app14020850.

[8] Kantzidis, P., Böhnisch, N., Masarati, P., and Muscarello, V., "About the Stabilizing Effect of the Torque on Propeller Whirl Flutter," *VFS 80th Annual Forum*, 2024.

[9] Bennett, R. M., and Bland, S. R., "Experimental and analytical investigation of propeller whirl flutter of a power plant on a flexible wing," Tech. Rep. NASA-TN-D-2399, NASA Langley Research Center, 1964.

[10] Böhnisch, N., Braun, C., Koschel, S., and Marzocca, P., "A Building-Block Approach to Study Aeroelastic Instabilities for Unconventional Aircraft Configurations," *AIAC 2021: 19th Australian International Aerospace Congress*, edited by Engineers Australia, 2021, pp. 160–166.

[11] Böhnisch, N., Braun, C., Muscarello, V., and Marzocca, P., "About the Wing and Whirl Flutter of a Slender Wing–Propeller System," *Journal of Aircraft*, 2024, pp. 1–14. doi: 10.2514/1.C037542.

[12] Teixeira, P. C., and Cesnik, C. E., "Propeller Influence on the stability of HALE Aircraft," *31st Congress of the International Council of the Aeronautical Sciences*, edited by ICAS, 9-14 September 2018.

[13] Böhnisch, N., Braun, C., Koschel, S., Muscarello, V., and Marzocca, P., "Dynamic Aeroelasticity of Wings with Distributed Propulsion System Featuring a Large Tip Propeller," *International Forum on Aeroelasticity and Structural Dynamics 2022*, 2022.

[14] Quanglong, C., Jinglong, H., and Haiwei, Y., "1084. Effect of engine thrust on nonlinear flutter of wings," *Vibroengineering: Journal of Vibroengineering*, Vol. 15, No. 4, 2013.

[15] Amoozgar, M., Hall, M., Dimitriadis, G., and Cooper, J. E., "The Effect of Thrust Vectoring on Aeroelastic Stability of Electric Aircraft," *AIAA SciTech Forum 2024*, 2024. doi:10.2514/6.2024-2044.

[16] Guruswamy, G. P., "Dynamic Aeroelasticity of Wings with Tip Propeller by Using Navier–Stokes Equations," *AIAA Journal*, Vol. 57, No. 8, 2019, pp. 3200–3205. doi:10.2514/1.J058610.

[17] Chang, J. C., Sanghi, D., and Cesnik, C. E. S., "Wing and Propeller Aerodynamic Interaction Effects on Whirl Flutter Instability," *VFS 80th Annual Forum*, 2024. doi: 10.13140/RG.2.2.30856.02561.

[18] Böhnisch, N., Braun, C., Muscarello, V., and Marzocca, P., "A Sensitivity Study on Aeroelastic Instabilities of Slender Wings with a Large Propeller," *AIAA SciTech 2023 Forum*, 2023. doi:10.2514/6.2023-1893.

[19] Rodden, W. P., and Rose, T. L., "Propeller/Nacelle Whirl Flutter Addition to MSC/NASTRAN," Tech. rep., The MacNeaI-Schwendler Corporation, 1989.

[20] Böhnisch, N., Braun, C., Muscarello, V., and Marzocca, P., "On the Suitability of Conventional Methods for the Aeroelastic Analysis of Novel Aircraft with Distributed Propulsion Systems," *AIAC 2023: 20th Australian International Aerospace Congress*, edited by Engineers Australia, 2023, pp. 51–56.

[21] Masarati, P., Morandini, M., and Mantegazza, P., "An Efficient Formulation for General-Purpose Multibody/Multiphysics Analysis," *Journal of Computational and Nonlinear Dynamics*, Vol. 9, No. 4, 2014. doi:10.1115/1.4025628.

[22] Zanotti, A., Savino, A., Palazzi, M., Tugnoli, M., and Muscarello, V., "Assessment of a Mid-Fidelity Numerical Approach for the Investigation of Tiltrotor Aerodynamics," *Applied Sciences*, Vol. 11, No. 8, 2021, p. 3385. doi:10.3390/app11083385.

[23] Pitt, D. M., and Peters, D. A., "Rotor Dynamic Inflow Derivatives and Time Constants from Various Inflow Models," *9th European Rotorcraft Forum*, Vol. Paper No. 55, 1983.

[24] Pitt, D. M., and Peters, D. A., "Theoretical prediction of dynamic inflow derivatives," *6th European Rotorcraft and Powered Lift Aircraft Forum*, 1980.

[25] Chourdakis, G., Davis, K., Rodenberg, B., Schulte, M., Simonis, F., Uekermann, B., Abrams, G., Bungartz, H. J., Cheung Yau, L., Desai, I., Eder, K., Hertrich, R., Lindner, F., Rusch, A., Sashko, D., Schneider, D., Totounferoush, A., Volland, D., Vollmer, P., and Koseomur, O. Z., "preCICE v2: A sustainable and user-friendly coupling library," *Open Research Europe*, Vol. 2, No. 51, 2022. doi:10.12688/openreseurope.14445.2.

[26] Savino, A., Cocco, A., Zanotti, A., Tugnoli, M., Masarati, P., and Muscarello, V., "Coupling Mid-Fidelity Aerodynamics and Multibody Dynamics for the Aeroelastic Analysis of Rotary-Wing Vehicles," *Energies*, Vol. 14, No. 21, 2021, p. 6979. doi:10.3390/en14216979.

[27] Reed, W. H., "Review of Propeller-Rotor Whirl Flutter," Tech. Rep. NASA TR R-264, NASA Langley Research Center, 1967.

[28] Veldhuis, L. L. M., "Propeller Wing Aerodynamic Interference," Ph.D. thesis, Delft University of Technology, Delft, The Netherlands, 2005.

[29] Aref, P., Ghoreyshi, M., Jirasek, A., Satchell, M., and Bergeron, K., "Computational Study of Propeller–Wing Aerodynamic Interaction," *Aerospace*, Vol. 5, No. 3, 2018, p. 79. doi:10.3390/aerospace5030079.

COPYRIGHT STATEMENT